



# Ammonium-driven nitrification and methane-driven denitrification achieve simultaneous nitrogen and metal removal in anaerobically digested sludge

Chenkai Niu<sup>a</sup>, Jianhua Guo<sup>a</sup>, Shihu Hu<sup>a</sup>, Tao Liu<sup>a,b,\*</sup>

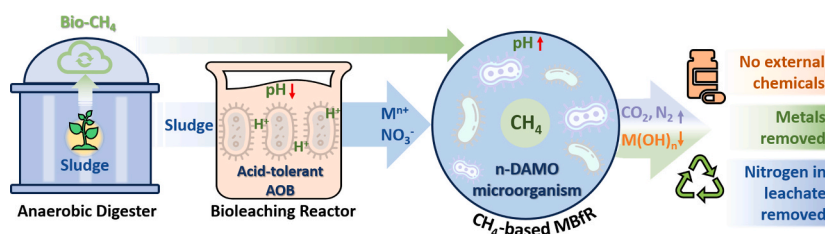
<sup>a</sup> Australian Centre for Water and Environmental Biotechnology (ACWEB, formerly AWMC), The University of Queensland, St. Lucia, Queensland 4072, Australia

<sup>b</sup> Department of Civil and Environmental Engineering, The Hong Kong Polytechnic University, Hung Hom, Kowloon 999077, Hong Kong, China

## HIGHLIGHTS

- Nitrification-driven bioleaching solubilized metals from anaerobically digested sludge.
- Methane-based denitrification removed nitrogen and enabled metal precipitation.
- Endogenous ammonium and methane enabled integrated nitrogen and metal management.
- The biological route reduced treatment cost by 57% compared with chemical methods.

## GRAPHICAL ABSTRACT



## ARTICLE INFO

### Keywords:

Acid-tolerant AOB  
Bioleaching  
Metals removal  
n-DAMO  
MBfR

## ABSTRACT

As a major sink of heavy metals, wastewater sludge requires management to avoid environmental and health risks, while conventional treatments (e.g. chemical leaching and precipitation) remain dependent on chemical additives. Leveraging the alkalinity variations inherent to nitrification and denitrification, we present a fully biological, chemical-free strategy for solubilizing metals from sludge to leachate, and subsequent elimination in the leachate together with nitrogen. In the first stage, nitrification, driven primarily by acid-tolerant ammonia-oxidizing bacteria (AOB), oxidized ammonium, consuming sludge alkalinity and reducing sludge pH to ~2.0, enabling efficient metals solubilization (Cu 85.6%, Zn 95.2%, Mn 85.2%, Al 73.5%). In the second stage, the acidic leachate underwent further treatment in a continuous methane-based membrane biofilm reactor (MBfR) enriched with nitrite/nitrate-dependent anaerobic methane-oxidizing (n-DAMO) microorganisms ('*Ca. Methylomirabilis*': 1.41% and '*Ca. Methanoperedens*': 2.34%). This process removed > 98.0% of total nitrogen at a rate of 753.3 ± 31.1 mg N/(L d). Due to the alkalinity produced during denitrification, the pH of MBfR was automatically raised to ~8.0, facilitating > 95.0% precipitation of solubilized metals. This work demonstrates a novel technical pathway for sludge management utilizing new nitrogen-cycling microorganisms and abundant nitrogen embedded in sludge, offering an environmentally sustainable pathway for integrated nitrogen and metal management in wastewater sludge.

\* Corresponding author at: Australian Centre for Water and Environmental Biotechnology (ACWEB, formerly AWMC), The University of Queensland, St. Lucia, Queensland 4072, Australia.

E-mail address: [tao1liu@polyu.edu.hk](mailto:tao1liu@polyu.edu.hk) (T. Liu).

<https://doi.org/10.1016/j.biortech.2026.134762>

Received 22 December 2025; Received in revised form 27 April 2026; Accepted 29 April 2026

Available online 30 April 2026

0960-8524/© 2026 The Author(s). Published by Elsevier Ltd. This is an open access article under the CC BY license (<http://creativecommons.org/licenses/by/4.0/>).

## 1. Introduction

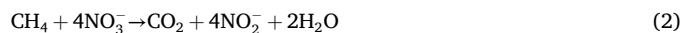
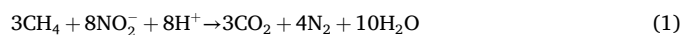
Sludge, a by-product of wastewater treatment, often contains large quantities of heavy metals that accumulate over time (Demirbas et al., 2017; Lake et al., 1984; Smith, 2009). These metals pose serious risks to both environmental and human health due to their toxicity and long-term persistence (Chu et al., 2022; Islam et al., 2017; Tou et al., 2017; Yakamercan et al., 2021). Specifically, when inadequately treated sludge is disposed of in landfills, heavy metals can leach into surrounding soils, disrupting soil structure, impairing fertility, and reducing crop productivity (Ansari et al., 2022; Bisht et al., 2024; Zhang et al., 2017). Furthermore, heavy metals absorbed by plants may enter the food chain, thereby threatening ecosystem stability (Angon et al., 2024; Kumar et al., 2019). Atmospheric emissions of heavy metals during sludge drying or incineration further exacerbate the environmental burden through air pollution (Law and Gordon, 1979; Wang et al., 2020; Zhang et al., 2013). Consequently, the effective removal of heavy metals from sludge has become an urgent environmental priority.

Heavy metals in contaminated sludge are commonly solubilized through chemical leaching using strong acids, which disrupt the bonds between metals and the sludge matrix (Camargo et al., 2016). Alternatively, bioleaching, usually facilitated by acidophilic iron- and sulfur-oxidizing bacteria, achieves similar outcomes via microbial metabolism that generates acids from compounds such as  $\text{FeSO}_4$ ,  $\text{FeS}_2$ , and elemental sulfur (Blais et al., 1993; Chen et al., 2022; Pathak et al., 2009). Both chemical and biological leaching effectively mobilize metals into the liquid phase, but they share a common drawback: reliance on externally added chemicals to drive the process. Another recently developed bioleaching approach uses ammonium inherently present in sludge (Wang et al., 2024), during which the microbial ammonium oxidation releases protons to enable bioleaching without the need for exogenous chemical inputs (Wang et al., 2021b). However, all the above leaching processes essentially transfer metals from the solid phase to the leachate without achieving true removal, leaving metal-laden supernatants that pose ongoing environmental risks. To achieve ultimate metal removal from wastewater systems, subsequent metal precipitation, typically by neutralization with alkaline agents such as quicklime, is employed to convert dissolved metal ions into insoluble hydroxides for removal and potential reuse (A. AbiD et al., 2011; Benalia et al., 2022; Bhattacharyya et al., 1979). Nevertheless, this step once again heavily depends on chemical inputs, limiting its sustainability.

Here, we propose a two-step bioprocess aimed at achieving effective metals removal from wastewater sludge, leveraging the alkalinity consumption and production during nitrification and denitrification, respectively. In the first stage, we employ nitrification primarily driven by acid-tolerant ammonia-oxidizing bacteria (AOB) to oxidize ammonium present in sludge, leading to the production of nitrate and a significant drop in sludge pH to  $\sim 2.0$ , which promotes the leaching of metals into the liquid phase (Wang et al., 2024). In the second stage, the metal- and nitrate-rich leachate is introduced into a denitrifying bioreactor. The denitrification process will increase the pH, favouring the bioprecipitation of heavy metals and simultaneously removing nitrogen from the sludge leachate.

Regarding the second stage of denitrification, adding external organics is straightforward but will lead to additional costs and potential secondary pollution with residual organics in effluent. Methane produced from the upstream sludge anaerobic digestion (AD) can potentially serve as a cheaper carbon source than traditional organic carbon for denitrification (Liu et al., 2019). A novel pathway that could use methane ( $\text{CH}_4$ ) as electron donors for denitrification involves the nitrite/nitrate-dependent anaerobic methane oxidation (*n*-DAMO) process (Zhang et al., 2024). Over the past decade, two distinct microbial groups have been identified in this process: ‘*Candidatus* Methanoperedens nitroreducens’ (*n*-DAMO archaea), which oxidize methane while reducing nitrate to nitrite, and ‘*Candidatus* Methyloirabilis oxyfera’ (*n*-DAMO bacteria), which further reduce nitrite to dinitrogen gas using

$\text{CH}_4$  as the electron donor (Eqs. (1) and (2)) (Ettwig et al., 2010; Haroon et al., 2013; Raghoebarsing et al., 2006). Notably, the activity of *n*-DAMO bacteria consumes protons, leading to a gradual increase in pH within the reactor (Liu et al., 2021; Lu et al., 2024). Although this pH elevation is often considered a challenge for maintaining optimal microbial activity, it may be leveraged to initiate the precipitation of solubilized heavy metals, offering a sustainable route for metal removal. To date, the integration of ammonium-driven bioleaching with  $\text{CH}_4$ -dependent *n*-DAMO-based denitrification for simultaneous metal precipitation and nitrogen removal has never been explored. This study demonstrates the feasibility of coupling these two processes in a two-stage system.



This study aimed to validate the feasibility of this two-stage system at the laboratory scale. A sequencing batch reactor (SBR), inoculated with acid-tolerant AOB (‘*Ca. Nitrosoglobus*’), was used to achieve nitrification-driven bioleaching of metals from AD sludge to leachate, as the first stage. The produced leachate containing heavy metals and nitrate was treated by a downstream  $\text{CH}_4$ -based membrane biofilm reactor (MBfR) as the second stage. The nitrogen removal and variations of metals in the sludge and leachate of both SBR and MBfR were closely monitored. Precipitated solids were characterized by SEM-EDS and XRD to elucidate metal speciation. Microbial community succession in MBfR was tracked via 16S rRNA gene amplicon sequencing, and functional batch assays confirmed the activity of *n*-DAMO archaea and bacteria in driving both nitrogen removal and pH increase. By integrating  $\text{CH}_4$  utilization, nitrogen removal, and metal removal in a continuous treatment train, this work demonstrates an integrated approach for wastewater sludge management, with implications for resource-oriented treatment strategies.

## 2. Materials and methods

### 2.1. Bioreactor setup and operation

#### 2.1.1. Nitrification-based bioleaching reactor

A lab-scale SBR was established (Fig. 1A), with a working volume of 1 L, to conduct metal leaching experiments in a temperature-controlled room at  $22 \pm 1^\circ\text{C}$ . All bioleaching experiments were conducted in 11 independent replicates under identical operational conditions. Before each experiment, 0.5 L of acid-tolerant AOB-enriched culture obtained from the Luggage Point wastewater treatment plant in Brisbane, Australia, was thoroughly mixed with 0.5 L of AD sludge. Each bioleaching run was initiated independently using freshly prepared inoculum but followed the same experimental protocol. The reactors were inoculated with acid-tolerant AOB culture sourced from a pilot-scale enrichment reactor at the Luggage Point Wastewater Treatment Plant (Brisbane, Australia), which has been continuously operated at  $\text{pH} < 5.0$  with stable partial nitrification performance. AD sludge was collected from the anaerobic digester of the same plant one day prior to the start of each run. No external acid, alkali, or buffer was added for pH control; the pH decrease during bioleaching was solely driven by biologically generated protons from ammonia oxidation. The basic properties of AOB culture and AD sludge could be found in Tables S1 and S2. Air was continuously supplied into the reactors, and magnetic stirrers were set to operate at 500 rpm. Given that the nitrogen in the AD sludge was sufficient to sustain the nitrification process, no additional nutrients were supplied. Throughout the bioleaching process, pH levels were monitored daily until the pH dropped to 2.0–3.0. Simultaneously, mixed sludge samples were collected to measure the concentrations of ammonium, nitrite, and nitrate. The metal solubilization efficiency was calculated based on the initial metal concentrations in the inoculum mixture and the concentration at the end of the leaching process. The sludge after the

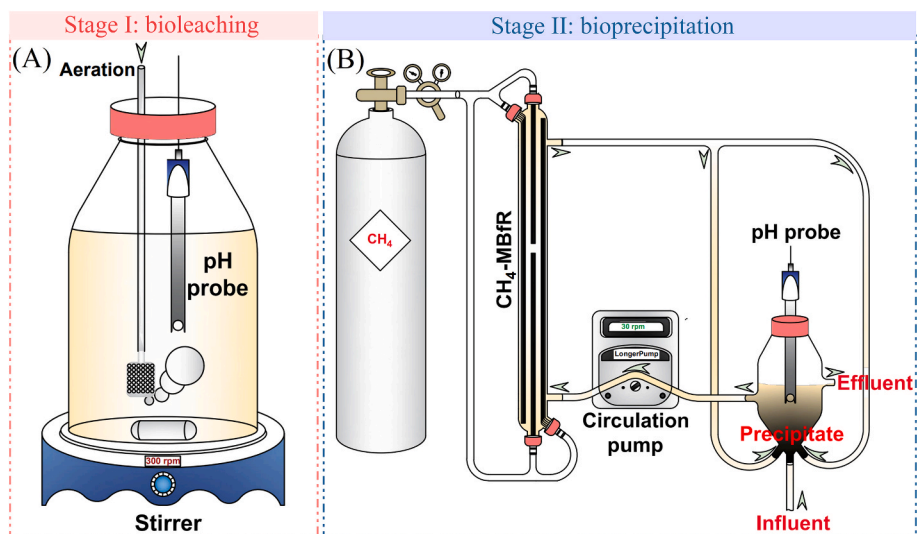


Fig. 1. Schematic of bioleaching reactor (A) and CH<sub>4</sub>-based MBfR (B).

bioleaching process was centrifuged at 4000 rpm (TD 6, Australia) for 15 min to separate the supernatant, which contained dissolved metal ions and nitrate. The supernatant was subsequently used as the feeding for the CH<sub>4</sub>-based MBfR.

### 2.1.2. CH<sub>4</sub>-based MBfR

A lab-scale MBfR with a working volume of 90 mL was set up to perform nitrogen removal and dissolved metal ions precipitation. As shown in Fig. 1B, three bundles of hollow fiber membranes (Model MHF-200TL, Mitsubishi, Ltd., Japan) were housed inside the MBfR. CH<sub>4</sub> was supplied from one end of the membranes, with the opposite end sealed to improve gas delivery efficiency. The CH<sub>4</sub> flow was controlled using a gas-pressure valve, maintaining a partial pressure of 4 psi. An overflow bottle was connected to the MBfR for sampling and pH monitoring. The overflow bottle was cone-shaped, allowing the collection of precipitated metals at the bottom and the recirculation of liquid via a circulating pump (BT100-2 J, Longerpump, Hebei, China). The long-term operation of the CH<sub>4</sub>-based MBfR consisted of three phases. In Phase I (Day 0–90), the primary goals were the establishment of biofilm and the enrichment of *n*-DAMO microorganisms. On Day 1, 40 mL of *n*-DAMO microorganism-containing suspension was inoculated into the MBfR. For the first seven days, the reactor operated in batch mode to prevent biomass loss. A nitrate stock solution (10 g N/L) was manually added to the MBfR, supporting microbial growth. After this initial period, the reactor was switched to continuous mode, fed with synthetic wastewater containing approximately 600 mg NO<sub>3</sub>-N/L and 100 mg NH<sub>4</sub><sup>+</sup>-N/L. The pH of the synthetic influent during this start-up stage was maintained at acidic pH conditions (pH < 4.0) by dosing 1 M HCl to mimic the acidic characteristics of leachate generated from the real bioleaching process. The medium composition was described in Table S3. The HRT was gradually reduced from five days to one day as bioactivity increased. In Phase II (Days 91–147), real bioleaching supernatant collected from the bioleaching SBR was introduced as the influent, expecting to achieve simultaneous metal and nitrogen removal. To minimize the impact of abrupt changes in influent pH on the MBfR, the bioleaching process was terminated at a final pH of approximately 3.0, which is slightly higher than the reported optimal bioleaching pH of ~ 2.0. The HRT was also extended to 3 days, and the total nitrogen concentration in the influent remained around 800 mg N/L. This temporary increase in HRT was intentionally implemented to buffer the transition from synthetic wastewater to real bioleaching leachate, which contained a more complex matrix with elevated metal concentrations and potential inhibitory components. Extending the HRT allowed gradual acclimation of the MBfR biofilm to the real leachate and minimized the risk of process

perturbation during this transition. In Phase III (Days 148–297), the MBfR was fed with real bioleaching leachate at a further reduced pH of approximately 2.0, and the HRT was gradually shortened to one day. External acid was only used during the start-up phase to prepare the synthetic influent for the MBfR, whereas no chemical reagents were applied throughout the subsequent bioleaching and bioprecipitation processes. Additional details of the key operating conditions are provided in Table S5. Nitrogen compound concentrations (nitrite, nitrate, and ammonium) in the effluent were measured three times per week, and the pH of the MBfR was regularly monitored during the long-term operation.

### 2.2. In situ batch assays to determine the activities of *n*-DAMO bacteria and *n*-DAMO archaea

After long-term operation, *in situ* batch tests were conducted to separately quantify the contributions of *n*-DAMO archaea (Batch A) and *n*-DAMO bacteria (Batch B). Prior to the batch assays, the continuous influent was halted, and fresh medium was used to flush both the CH<sub>4</sub>-based MBfR and its overflow bottle to remove any residual substrates. In Batch A, sodium nitrate (5 g/L) was introduced into the MBfR, resulting in an initial nitrate concentration of approximately 30 mg N/L. Samples were then collected from the overflow bottle, and the activity of *n*-DAMO archaea was determined by calculating the volumetric nitrate reduction rate. For Batch B, the same flushing procedure was followed, after which sodium nitrite (5 g/L) was added to achieve a starting nitrite concentration of approximately 30 mg N/L. The activity of *n*-DAMO bacteria was assessed based on the volumetric nitrite removal rate. Each assay was conducted for 1 h and performed in triplicate, with liquor samples collected every 15 min to monitor nitrogen profiles.

### 2.3. Characterization of metal precipitates

Precipitated samples collected from the bottom of the overflow bottle were prepared for SEM-EDS analysis. The samples underwent a series of dewatering, drying, and coating steps prior to SEM observation using a JEOL JSM-7100F (Japan). The samples were dehydrated through a series of ethanol or acetone washes, with gradually increasing concentrations (e.g., 30%, 50%, 70%, 90%, 100%) to effectively remove water. Following dehydration, the samples were air-dried to eliminate any residual solvent without causing structural collapse. The dried samples were mounted onto aluminum SEM stubs using conductive adhesive tape to securely position them for imaging. The samples were then sputter-coated with a thin layer of platinum to prevent charging

under the electron beam and to enhance the imaging signal. After preparation, the samples were transferred to the SEM chamber, where imaging was conducted under either high vacuum or low vacuum conditions, depending on the requirements of the analysis. X-ray diffraction (XRD) analysis was conducted to characterize the crystalline features of the precipitated solids. The samples were air-dried and gently ground prior to analysis. XRD patterns were collected using a Bruker D8 Advance powder X-ray diffractometer operated in Bragg–Brentano geometry. Measurements were performed at room temperature (25°C) using Co K $\alpha$  radiation with an energy-dispersive detector. Data were acquired in a coupled  $\theta$ – $2\theta$  scanning mode over a  $2\theta$  range of 5–90°, with a step size of 0.020° and a counting time of 1.0 s per step.

#### 2.4. DNA extraction and 16S rRNA gene amplicon sequencing

Biofilm samples from the seeding sludge, Day 62, and Day 286 were collected. DNA extraction was performed using the FastDNA SPIN Kit for Soil (MP Biomedical, USA) according to manufacturer's protocol. Since no suspended biomass existed in the overflow bottle, biofilm was randomly taken from the MBfR and then mixed well to create a representative biomass for DNA extraction. Biomass samples were not collected from the bioleaching reactors, as it was a batch reactor with each cycle lasting within 14 days, and the functional nitrifying microorganism was assumed to have minor changes. To analyze the microbial community composition, universal primers 926F (5'-AAACTYAAK-GAATTGACGG-3') and 1392R (5'-ACGGGCGGTGTGTRC-3') were used to amplify the V6 to V8 regions of the 16S rRNA gene. The sequencing was conducted on the DNBSEQ-G400 platform. The raw sequencing data were filtered to obtain high-quality clean data, which were then merged into tags and subsequently clustered into operational taxonomic units (OTUs) (Kong et al., 2024; Li et al., 2023).

#### 2.5. Chemical analysis

Sludge/liquid samples obtained from the influent/effluent of bioleaching reactors and CH $_4$ -based MBfR were filtered through a 0.22  $\mu$ m membrane to remove particles. Nitrate, nitrite and ammonium concentrations were determined using a Flow Injection Analyzer (Lachat QuickChem8000, Lachat Instrument, Milwaukee, WI). Metal ions concentrations were quantified using Inductively Coupled Plasma-Optical Emission Spectrometry (ICP-OES) (Thermo Scientific iCAP 7000 plus Series, U.S.). For the metals in sludge, 5 mL of the sludge sample was digested with 5 mL of 70% HNO $_3$  at 200°C for 30 min in a microwave digestion system (MARS 6, USA). The digestion process involved a 15-minute ramp from room temperature to 200°C, followed by a 15-minute hold at 200°C. The resulting solution was analyzed using ICP-OES to measure the total metal concentration. To determine the concentration of dissolved metals, the mixture was first centrifuged at 13,000 rpm for 15 min. The supernatant was then filtered using a sterile 0.45  $\mu$ m Millipore filter (SLLHR04NL, Merck, USA). Subsequently, 3.6 mL of the supernatant was mixed with 0.4 mL of 70% HNO $_3$  and digested at 160°C for 20 min (10 min to reach 160°C, followed by 10 min at 160°C). The metal solubilization efficiency of AD sludge and the metal removal efficiency were calculated based on the total metal concentration in sludge, metal concentrations in the supernatant after the bioleaching process and metal concentrations in effluent of the MBfR (Liu et al., 2023a).

### 3. Results and Discussion

#### 3.1. Release of metals from AD sludge via nitrification-based bioleaching

Bioleaching of metals was accomplished by mixing AD sludge, rich in ammonium and metals, with the acid-tolerant AOB culture, which can metabolize and thrive in extreme pH environments (Hayatsu et al., 2017; Wang et al., 2021a). Under aerobic conditions, the nitrification

process, primarily driven by acid-tolerant AOB, oxidized ammonia into nitrate, generating protons that acidified the sludge (Li et al., 2020; Meng et al., 2022). This acidification process typically persisted for 9 to 14 days, ultimately reducing the pH to approximately 2.0. This approach is notably distinct from traditional chemical leaching methods, which require the addition of significant amounts of external inorganic acids, incurring high operational costs and risks of secondary pollution from residual chemicals (Liang et al., 2019; Wang et al., 2018). Similarly, conventional bioleaching methods are often accompanied by the addition of Fe and S agents, which further complicates the process (Liu et al., 2015; Pathak et al., 2009). In contrast, the nitrification-based bioleaching demonstrated here is driven entirely by endogenous NH $_4^+$  present in the sludge matrix, requiring only aeration and mixing, thereby substantially reducing chemical input and operational complexity.

As demonstrated in Fig. 2A, the four targeted metals (Cu, Zn, Mn and Al) were efficiently solubilized into the liquid phase when the sludge pH decreased to  $\sim$ 2.0, with an overall solubilization efficiency exceeding 85%. Specifically, the solubilization efficiencies for Cu, Zn, Mn, and Al were 85.6  $\pm$  2.6%, 95.2  $\pm$  2.4%, 85.2  $\pm$  2.6%, and 73.5  $\pm$  2.1%, respectively. The relatively lower solubilization efficiency of Al is likely due to its stable chemical properties and its competitive interactions with other metals (Gensemer and Playle, 1999). Additionally, the solubilization efficiencies of five other toxic metals were determined, with Ni exhibiting the highest efficiency (Fig. S1). The correlation between the end-point pH and the residual NH $_4^+$ /generated NO $_3^-$  in the bioleaching process was illustrated in Fig. 2B. Specifically, when a lower end-point pH in the bioleaching process was set, more protons were required. Based on the first step of nitrification (NH $_4^+$  + 1.5 O $_2$   $\rightarrow$  NO $_2^-$  + 2H $^+$  + H $_2$ O), more ammonium was oxidized, leaving less in the bioleaching supernatant. As the pH decreased from 2.86 to 2.03, the proportion of nitrate increased substantially, while the ammonium concentration declined. However, this first stage primarily transfers metals from the solid sludge phase into the liquid leachate. If the leachate were returned to the mainstream wastewater treatment stream, as is commonly practised, the solubilized metals would be reintroduced into the system and ultimately reaccumulated in the sludge (Babel and del Mundo Dacera, 2006). This limitation necessitates a second treatment stage for effective metal removal from the leachate, which is addressed by the downstream CH $_4$ -based MBfR. Following bioleaching, the supernatant containing dissolved metal ions and nitrate was introduced into the CH $_4$ -based MBfR for simultaneous nitrogen removal and metal ions precipitation.

#### 3.2. Nitrogen removal from leachate in CH $_4$ -based MBfR

In the biofilm establishment and *n*-DAMO microorganism enrichment stage (Day 0–90), synthetic wastewater with around 600 mg N/L of nitrate and 100 mg N/L of ammonium was prepared as influent. The HRT was initially set for 5 days following the transition to continuous feeding and was gradually reduced to 1 day after 27 days of operation (Fig. 3A). The influent pH was manually adjusted to below 3.0 to simulate real bioleaching supernatant, allowing the microorganisms to acclimatize to highly acidic feeding. Due to proton consumption by the *n*-DAMO bacteria, the effluent pH (which is identical to the pH in the continuous MBfR) increased to an alkaline range, between 7.5 and 8.5. Nitrate was completely reduced by *n*-DAMO archaea, and the nitrite produced was subsequently removed by *n*-DAMO bacteria, leaving only ammonium in the effluent (71.3  $\pm$  22.5 mg N/L) (Fig. 3B).

On Day 91, during Phase II, real bioleaching leachate was introduced into the MBfR, and the HRT was extended to 3 days to mitigate the potential negative effects of the real wastewater on the microorganisms. Additionally, the final pH of the upstream bioleaching process was controlled to be  $\sim$  3.0, also to avoid potential inhibition to the microorganisms in MBfR. As expected, the effluent pH still stabilized at approximately 7.5, facilitating the precipitation of metal ions. While

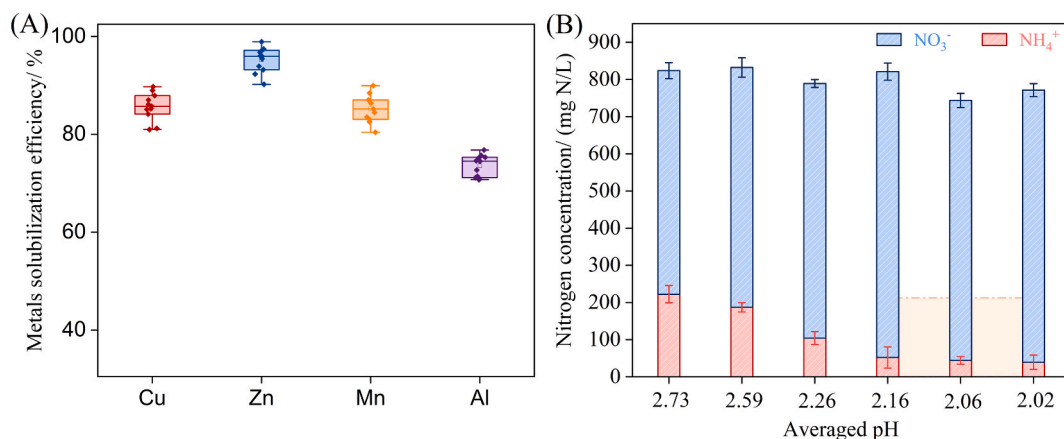


Fig. 2. Bioleaching results. (A) Solubilization efficiency of representative metals in 11 independent SBR cycles. (B) Correlation between the end-point pH and nitrogenous compounds in the bioleaching reactor. Bars and symbols represent mean  $\pm$  SD (n = 11).

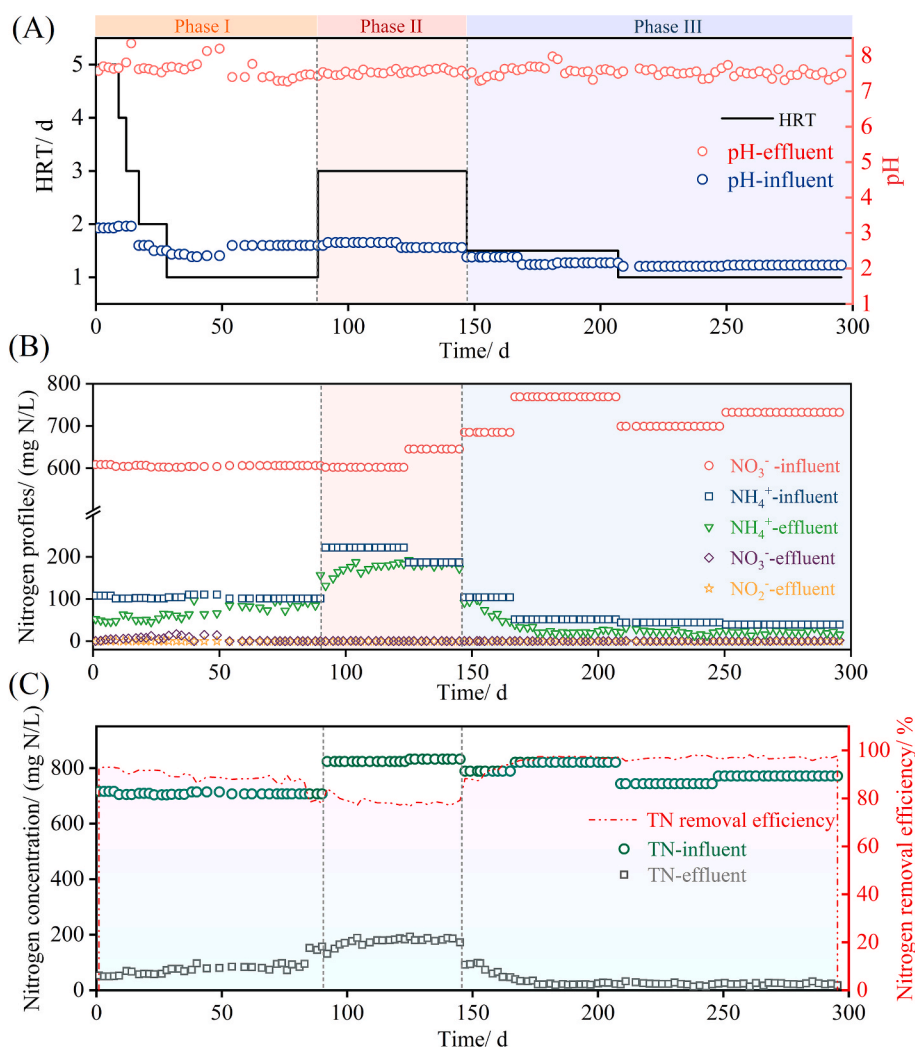


Fig. 3. Nitrogen removal performance of the  $\text{CH}_4$ -based MBfR. (A) HRT and pH levels in the influent and effluent; (B) Nitrogen concentrations in the influent and effluent of the MBfR; (C) TN concentration and its removal efficiency.

nitrate was completely removed without nitrite accumulation, the effluent ammonium concentration increased to  $172.5 \pm 21.4$  mg N/L, and the corresponding total nitrogen removal efficiency decreased to approximately 80% during Phase II. This elevated ammonium level, compared to the previous stage, was attributed to the higher influent

ammonium concentration associated with an influent pH of  $\sim 3.0$  (Fig. 2B). Specifically, this observation suggests that a bioleaching end-point pH of  $\sim 3.0$  was insufficient to fully consume ammonium released from the sludge matrix, leading to  $\text{NH}_4^+$  carryover into the downstream MBfR and necessitating further process optimization in Phase III.

Since the acidic pH of 3.0 in the real leachate did not compromise MBfR performance, the final pH of the upstream bioleaching process was adjusted to approximately 2.0 in Phase III. This adjustment not only enhanced metal solubilization during bioleaching but also significantly reduced the influent ammonium concentration (Fig. 3B). Promisingly, regardless of the variations of influent pH, the effluent pH remained stable at around 7.5. With enhanced microbial activities (no nitrate or nitrite accumulation in effluent), the HRT gradually dropped back to 1 d. Regarding nitrogen profiles, no nitrate was detected in the effluent, and the residual ammonium concentration gradually decreased, reaching approximately 25 mg N/L from Day 153 onwards. As a result of the decreased ammonium levels in the effluent, the total nitrogen removal efficiency increased to 98% at a rate of  $753.3 \pm 31.1$  mg N/(L·d) during Phase III. This leverages the unique capacity of *n*-DAMO microorganisms (Raghoebarsing et al., 2006) to utilize methane produced from upstream sludge anaerobic digestion as the electron donor, effectively eliminating the need for external carbon sources and substantially reducing operational costs compared to conventional denitrification strategies. Previous studies have applied the *n*-DAMO process primarily for nitrogen removal and greenhouse gas mitigation, such as combining it with the Anammox process to remove ammonium, nitrate, nitrite, and dissolved methane (Liu et al., 2023a, 2023b). The present study expands the potential application scope of the *n*-DAMO process beyond conventional nitrogen removal by integrating it with downstream metal precipitation, as detailed in Section 3.3.

### 3.3. Precipitation of metal ions in CH<sub>4</sub>-based MBfR

Metals in the sludge (Cu, Zn, Mn and Al) were effectively solubilized through the nitrification-driven bioleaching process (Fig. 2A). Afterwards, the bioleaching leachate with soluble metal ions and nitrate undergoes denitrification by *n*-DAMO microorganisms within the CH<sub>4</sub>-based MBfR (Fig. 3). Simultaneously, the alkalinity generated during this process raised the pH to alkaline levels, thereby promoting the precipitation of metal ions in the leachate. The average precipitation efficiencies for Cu, Zn, Al, and Mn were  $99.4 \pm 0.5\%$ ,  $99.5 \pm 0.4\%$ ,  $98.6 \pm 0.4\%$ , and  $97.4 \pm 0.3\%$ , respectively, over the long-term operation of the MBfR (Fig. 4A). In addition to biologically induced alkalinity generation, minor contributions from physicochemical processes such as adsorption and abiotic precipitation may also be involved in metal removal. Furthermore, other toxic metals (Pb, Cd, As, Ni, etc.) were efficiently removed from the leachate, with removal efficiencies exceeding 80.0% for all elements (Fig. S2), further mitigating the risk of heavy metal pollution in the event of sludge land application.

To further verify the presence of the precipitated metal ions, SEM-EDS analysis was conducted on the solid particles collected from the conical bottom of the overflow bottle. The morphology of the precipitates is shown in Fig. 4B, where valuable metals such as Cu, Zn, and Al were detected, confirming the successful precipitation and removal of the target metals (Fig. 4C). The absence of other metal elements in the EDS signals could be attributed to their low concentrations in the bioleaching supernatant or the specific location of the EDS scan.

After confirming the presence of metal elements in the precipitated solids by EDS analysis, XRD was further employed to examine the crystalline characteristics of the metal-containing precipitates (Fig. 4D). Diffraction features associated with Cu- and Zn-containing phases were clearly observed, whereas elements present at lower concentrations in the sludge exhibited relatively weaker signals. For Cu, the observed diffraction features were consistent with the formation of Cu-associated hydroxide-like or hydrated metal phases. In contrast, the Zn-related diffraction features suggest the presence of more complex metal-associated phases, potentially involving co-precipitation with Fe and phosphate components. It should be noted that XRD alone does not allow definitive identification of specific chemical species; however, the observed patterns are consistent with metal precipitation occurring under the alkaline conditions generated during denitrification. In

addition, a broad and low-intensity diffraction feature centered around  $2\theta \approx 20^\circ$  was observed, attributed to amorphous organic matter originating from biomass-derived components (e.g., C-, N-, O-, and H-containing organic phases), rather than crystalline mineral phases. The broad and overlapping diffraction features further indicate that the precipitates were composed of mixed and poorly crystalline phases rather than well-defined single minerals.

The precipitated metal hydroxides obtained in this study may hold potential for recovery and reuse; however, given the co-precipitation of multiple metals and other components from the complex sludge matrix, further downstream separation, purification, and characterization would be required before any practical valorization, an aspect that warrants future investigation.

It is also worth acknowledging that, while the present study demonstrated effective metal removal from the aqueous phase, it did not include detailed examination of possible metal deposition or scaling on the membrane surface. In long-term operation, inorganic precipitation or bio-mineralization could potentially occur on the membrane, impairing mass transfer, promoting membrane fouling, and increasing operational costs. Membrane fouling risks may be mitigated by favoring bulk precipitation over surface deposition, operating at moderate gas pressure, and applying periodic gas-side cleaning when compatible with membrane materials. Future work should therefore incorporate advanced structural characterization, such as X-ray (Micro) Computed Tomography to visualize in situ biofilm thickness and metal accumulation, along with periodic monitoring of permeability and trans-membrane pressure to track performance changes over extended operation.

### 3.4. Variation of functional microorganisms

The influent of the CH<sub>4</sub>-based MBfR was switched from synthetic wastewater to real bioleaching leachate accompanied by subsequent pH adjustments. To assess the effects of these changes on *n*-DAMO microorganisms within the biofilm, 16S rRNA gene amplicon sequencing was employed. Biofilm samples were collected from the inoculum, Day 62 (Phase I, fed with synthetic wastewater), and Day 286 (Phase III, fed with bioleaching supernatant) for comparative analysis. As shown in the genus-level heatmap (Fig. 5A), the overall community structures in the inoculum and Phase II were highly similar, likely due to the short operational time and stable influent composition. In Phase III, prolonged exposure to the more complex bioleaching supernatant led to notable shifts in dominant taxa, with certain heterotrophic denitrifiers (e.g., *Pseudomonas*, *Proteiniphilum*) becoming more prevalent. This was accompanied by slight reductions in community evenness, suggesting that the selective pressure favored specific ecological guilds.

At the genus level (Fig. 5B), '*Ca. Methyloirabilis*' and '*Ca. Methanoperedens*' accounted for 0.35% and 0.78% of the inoculum, respectively, and increased to 0.83% and 1.09% by Day 62, indicating successful enrichment that supported a higher nitrogen removal capacity. After switching to bioleaching leachate for a prolonged period, their abundances only slightly varied despite the presence of potentially inhibitory compounds in the real wastewater. Indeed, their relative abundances further increased to 1.63% ('*Ca. Methanoperedens*') and 0.98% ('*Ca. Methyloirabilis*'), demonstrating the stability of the CH<sub>4</sub>-MBfR system and explaining the sustained high denitrification efficiency. Furthermore, batch test results (Fig. S3) at the end of Phase III confirmed high nitrate and nitrite reduction rates, 25.1 and 27.7 mg N/(L·h), respectively, which were higher than the values reported for *n*-DAMO microorganisms in most previous studies (Lim et al., 2021; Liu et al., 2023a), further underscoring the robust performance of the enriched biofilm community. While 16S rRNA analysis provides useful evidence to support the dominant microbial groups, taxonomy-based relative abundance does not constitute direct functional evidence. Functional validation and higher-resolution temporal sampling would be beneficial to strengthen the interpretation of microbial dynamics.

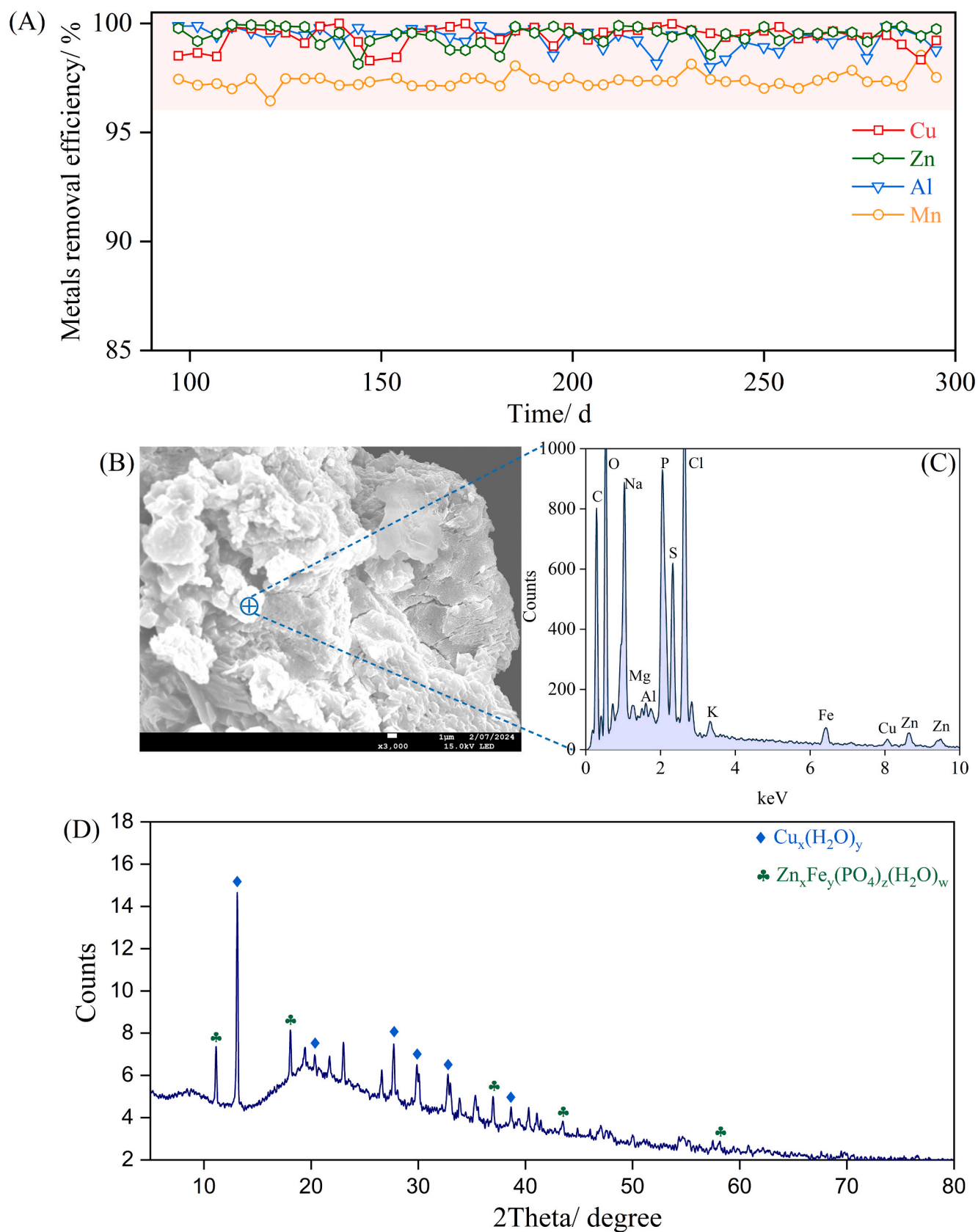


**Fig. 4.** The precipitation performance of metal ions in  $\text{CH}_4$ -based MBfR: (A) The removal efficiency of four representative metals; (B) The morphology of the metal precipitate; (C) The detected element signals from EDS; (D) XRD pattern of the precipitated solids, indicating the presence of metal-containing mineral phases.

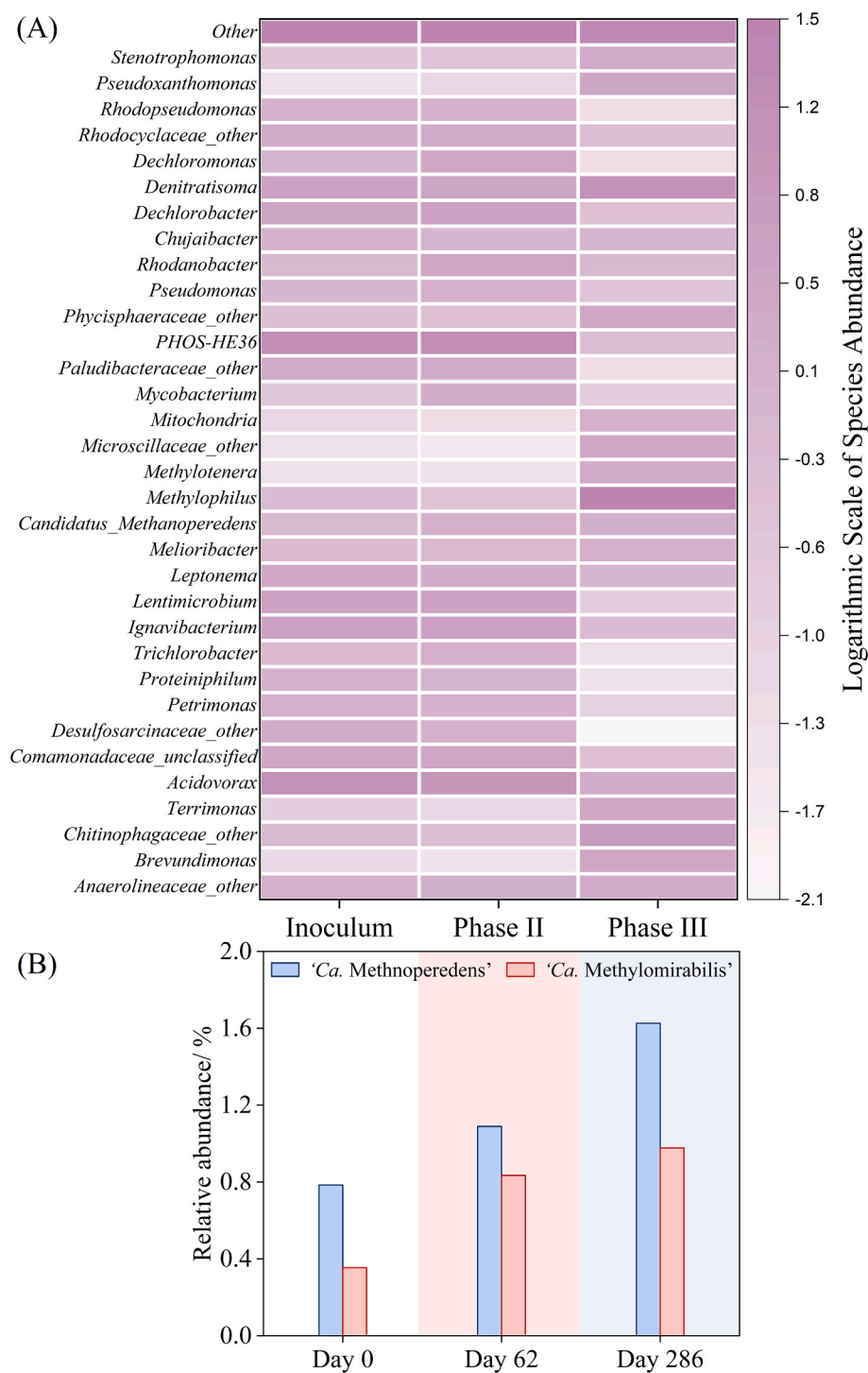


**Fig. 5.** Microbial communities in the CH<sub>4</sub>-based MBfR. (A) Taxonomic classification of bacterial communities at the genus level, showing only those with a relative abundance  $\geq 1.0\%$  in at least one sample. (B) Dynamics of *n*-DAMO related microorganisms during long-term operation of the CH<sub>4</sub>-based MBfR.

### 3.5. Economic perspective and process sustainability

From an economic perspective, the conventional strategy involving acid leaching with strong acids (e.g., HCl) followed by chemical precipitation with alkaline reagents (e.g., quicklime) incurs high reagent-related costs (Text S1). In contrast, the two-step biological process proposed in this study substantially reduces chemical input: bioleaching is driven by endogenous NH<sub>4</sub><sup>+</sup> in the sludge, requiring only aeration and mixing, while bioprecipitation is achieved in a CH<sub>4</sub>-based MBfR with CH<sub>4</sub> potentially sourced from biogas generated via anaerobic digestion

of the same sludge. Overall, the total treatment cost of the biological approach was estimated at \$38.11 per tonne of dry sludge, 57.0% lower than that of the chemical method (\$88.75, Table S4). This cost advantage, combined with the demonstrated nitrogen removal efficiency of up to 98% and metal precipitation efficiency exceeding 95%, highlights the overall potential of the integrated biological route as a more sustainable and cost-effective alternative for sludge metal management under the conditions investigated. Wastewater treatment plants generate significant amounts of sludge daily, which is abundant in essential nutrients such as nitrogen, phosphorus, and potassium, making its use as a land

fertilizer a viable option (Hu et al., 2022; Mailler et al., 2014). However, these facilities also concentrate substantial amounts of metal elements in the sludge (Babel and del Mundo Dacera, 2006), and if left untreated, these metals can enter the soil system upon sludge disposal, posing serious environmental and health risks. The integrated approach demonstrated in this study therefore simultaneously addresses metal removal for safer sludge utilization and nitrogen removal with resource recovery potential, representing a meaningful advancement toward more sustainable sludge management practices.

#### 4. Conclusions

This study demonstrates a two-step biological process integrating ammonium-driven nitrification with methane-dependent denitrification to simultaneously remove metals from anaerobically digested sludge and nitrogen from sludge digestion liquor. Nitrification-driven bioleaching by acid-tolerant AOB reduced sludge pH to ~2.0, achieving > 85% solubilization of Cu, Zn, Mn, and Al, while methane-dependent denitrification by *n*-DAMO microorganisms subsequently removed > 98% of nitrogen and raised the pH to ~8.0, enabling > 95% precipitation of the solubilized metals. The proposed route offers a sustainable strategy by relying primarily on endogenous ammonium in sludge and methane present in sludge treatment systems. In conclusion, this work presents a novel alternative for sludge treatment, and future research should focus on the reuse potential of recovered metal hydroxides to support its transition from laboratory feasibility to large-scale application.

#### CRedit authorship contribution statement

**Chenkai Niu:** Writing – original draft, Methodology, Formal analysis, Data curation. **Jianhua Guo:** Writing – review & editing, Conceptualization. **Shihu Hu:** Writing – review & editing, Project administration, Funding acquisition. **Tao Liu:** Writing – review & editing, Supervision, Funding acquisition, Conceptualization.

#### Declaration of competing interest

The authors declare that they have no known competing financial interests or personal relationships that could have appeared to influence the work reported in this paper.

#### Acknowledgements

This work is supported by Australian Research Council through Linkage Projects (LP220200963). Tao Liu acknowledges the support of the Hong Kong Research Grants Council Early Career Scheme (PolyU 25238324).

#### Appendix A. Supplementary data

Supplementary data to this article can be found online at <https://doi.org/10.1016/j.biortech.2026.134762>.

#### Data availability

Data will be made available on request.

#### References

- Abid, B., BrbootI, M., Al-ShuwaikI, N., 2011. Removal of heavy metals using chemicals precipitation. *ETJ* 29, 595–612. <https://doi.org/10.30684/etj.29.3.15>.
- Angon, P.B., Islam, M.S., Kc, S., Das, A., Anjum, N., Poudel, A., Suchi, S.A., 2024. Sources, effects and present perspectives of heavy metals contamination: soil, plants and human food chain. *Heliyon* 10. <https://doi.org/10.1016/j.heliyon.2024.e28357>.

- Ansari, M.S., Tauseef, A., Haris, M., Khan, A., Hussain, T., Khan, A.A., 2022. 12 - Effects of heavy metals present in sewage sludge, their impact on soil fertility, soil microbial activity, and environment. In: Shah, M.P., Rodriguez-Couto, S., Shah, N., Banerjee, R. (Eds.), *Development in Waste Water Treatment Research and Processes*. Elsevier, pp. 197–214. doi: 10.1016/B978-0-323-85584-6.00013-3.
- Babel, S., del Mundo Dacera, D., 2006. Heavy metal removal from contaminated sludge for land application: a review. *Waste Manag.* 26, 988–1004. <https://doi.org/10.1016/j.wasman.2005.09.017>.
- Benalia, M.C., Youcef, L., Bouaziz, M.G., Achour, S., Menasra, H., 2022. Removal of Heavy Metals from Industrial Wastewater by Chemical Precipitation: Mechanisms and Sludge Characterization. *Arab. J. Sci. Eng.* 47, 5587–5599. <https://doi.org/10.1007/s13369-021-05525-7>.
- Bhattacharyya, D., Jumawan Jr., A.B., Grieves, R.B., 1979. Separation of toxic Heavy Metals by Sulfide Precipitation. *Sep. Sci. Technol.* 14, 441–452. <https://doi.org/10.1080/01496397908058096>.
- Bisht, A., Kamboj, V., Kamboj, N., Bharti, M., Bahukahndi, K.D., Saini, H., 2024. Impact of solid waste dumping on soil quality and its potential risk on human health and environment. *Environ. Monit. Assess.* 196, 763. <https://doi.org/10.1007/s10661-024-12914-6>.
- Blais, J.F., Tyagi, R.D., Auclair, J.C., 1993. Bioleaching of metals from sewage sludge: Microorganisms and growth kinetics. *Water Res.* 27, 101–110. [https://doi.org/10.1016/0043-1354\(93\)90200-2](https://doi.org/10.1016/0043-1354(93)90200-2).
- Camargo, F.P., Sérgio Tonello, P., dos Santos, A.C.A., Duarte, I.C.S., 2016. Removal of toxic Metals from Sewage Sludge through Chemical, Physical, and Biological Treatments—a Review. *Water Air Soil Pollut.* 227, 433. <https://doi.org/10.1007/s11270-016-3141-3>.
- Chen, C., Li, H., Cui, F., Wang, Z., Liu, X., Jiang, G., Cheng, T., Bai, R., Song, L., 2022. Novel combination of bioleaching and persulfate for the removal of heavy metals from metallurgical industry sludge. *Environ. Sci. Pollut. Res.* 29, 33751–33763. <https://doi.org/10.1007/s11356-021-18068-z>.
- Chu, L., He, W., Xu, F., Tong, Y., Xu, F., 2022. Ecological risk assessment of toxic metal (oid)s for land application of sewage sludge in China. *Sci. Total Environ.* 836, 155549. <https://doi.org/10.1016/j.scitotenv.2022.155549>.
- Demirbas, A., Edris, G., Alalayah, W.M., 2017. Sludge production from municipal wastewater treatment in sewage treatment plant. *Energy Sources Part A* 39, 999–1006. <https://doi.org/10.1080/15567036.2017.1283551>.
- Ettwig, K.F., Butler, M.K., Le Paslier, D., Pelletier, E., Mangenot, S., Kuypers, M.M.M., Schreiber, F., Dutilh, B.E., Zedelius, J., de Beer, D., Gloerich, J., Wessels, H.J.C.T., van Alen, T., Luesken, F., Wu, M.L., van de Pas-Schoonen, K.T., Op den Camp, H.J.M., Janssen-Megens, E.M., Francoijs, K.-J., Stunnenberg, H., Weissenbach, J., Jetten, M.S.M., Strous, M., 2010. Nitrite-driven anaerobic methane oxidation by oxygenic bacteria. *Nature* 464, 543–548. <https://doi.org/10.1038/nature08883>.
- Geneser, R.W., Playle, R.C., 1999. The Bioavailability and Toxicity of Aluminum in Aquatic Environments. *Crit. Rev. Environ. Sci. Technol.* 29, 315–450. <https://doi.org/10.1080/1064338991259245>.
- Haroon, M.F., Hu, S., Shi, Y., Imelfort, M., Keller, J., Hugenholtz, P., Yuan, Z., Tyson, G. W., 2013. Anaerobic oxidation of methane coupled to nitrate reduction in a novel archaeal lineage. *Nature* 500, 567–570. <https://doi.org/10.1038/nature12375>.
- Hayatsu, M., Tago, K., Uchiyama, I., Toyoda, A., Wang, Y., Shimomura, Y., Okubo, T., Kurisu, F., Hirono, Y., Nonaka, K., Akiyama, H., Itoh, T., Takami, H., 2017. An acid-tolerant ammonia-oxidizing  $\gamma$ -proteobacterium from soil. *ISME J.* 11, 1130–1141. <https://doi.org/10.1038/ismej.2016.191>.
- Hu, J., Zhao, J., Zheng, X., Li, S., Lv, Q., Liang, C., 2022. Removal of heavy metals from sewage sludge by chemical leaching with biodegradable chelator methyl glycine diacetic acid. *Chemosphere* 300, 134496. <https://doi.org/10.1016/j.chemosphere.2022.134496>.
- Islam, M.S., Ahmed, M.K., Raknuzzaman, M., Habibullah-Al-Mamun, Md., Kundu, G.K., 2017. Heavy metals in the industrial sludge and their ecological risk: a case study for a developing country. *J. Geochem. Explor.* 172, 41–49. <https://doi.org/10.1016/j.gexplo.2016.09.006>.
- Kong, Z., Wang, Z., Lu, X., Song, Y., Yuan, Z., Hu, S., 2024. Significant *in situ* sludge yield reduction in an acidic activated sludge system. *Water Res.* 261, 122042. <https://doi.org/10.1016/j.watres.2024.122042>.
- Kumar, S., Prasad, S., Yadav, K.K., Shrivastava, M., Gupta, N., Nagar, S., Bach, Q.-V., Kamyab, H., Khan, S.A., Yadav, S., Malav, L.C., 2019. Hazardous heavy metals contamination of vegetables and food chain: Role of sustainable remediation approaches - a review. *Environ. Res.* 179, 108792. <https://doi.org/10.1016/j.envres.2019.108792>.
- Lake, D.L., Kirk, P.W.W., Lester, J.N., 1984. Fractionation, Characterization, and Speciation of Heavy Metals in Sewage Sludge and Sludge-Amended Soils: a Review. *J. Environ. Qual.* 13, 175–183. <https://doi.org/10.2134/jeq1984.00472425001300020001x>.
- Law, S.L., Gordon, G.E., 1979. Sources of metals in municipal incinerator emissions. *Environ. Sci. Technol.* 13, 432–438. <https://doi.org/10.1021/es60152a010>.
- Li, J., Liu, T., McLroy, S.J., Tyson, G.W., Guo, J., 2023. Phylogenetic and metabolic diversity of microbial communities performing anaerobic ammonium and methane oxidations under different nitrogen loadings. *ISME Commun.* 3, 1–10. <https://doi.org/10.1038/s43705-023-00246-4>.
- Li, J., Xu, K., Liu, T., Bai, G., Liu, Y., Wang, C., Zheng, M., 2020. Achieving Stable Partial Nitrification in an Acidic Nitrifying Bioreactor. *Environ. Sci. Technol.* 54, 456–463. <https://doi.org/10.1021/acs.est.9b04400>.
- Liang, S., Chen, H., Zeng, X., Li, Z., Yu, W., Xiao, K., Hu, J., Hou, H., Liu, B., Tao, S., Yang, J., 2019. A comparison between sulfuric acid and oxalic acid leaching with subsequent purification and precipitation for phosphorus recovery from sewage sludge incineration ash. *Water Res.* 159, 242–251. <https://doi.org/10.1016/j.watres.2019.05.022>.

- Lim, Z.K., Liu, T., Zheng, M., Yuan, Z., Guo, J., Hu, S., 2021. Versatility of nitrite/nitrate-dependent anaerobic methane oxidation (n-DAMO): first demonstration with real wastewater. *Water Res.* 194, 116912. <https://doi.org/10.1016/j.watres.2021.116912>.
- Liu, C., Liu, T., Zheng, X., Meng, J., Chen, H., Yuan, Z., Hu, S., Guo, J., 2021. Rapid formation of granules coupling n-DAMO and anammox microorganisms to remove nitrogen. *Water Res.* 194, 116963. <https://doi.org/10.1016/j.watres.2021.116963>.
- Liu, H., Xia, J., Nie, Z., 2015. Relatedness of Cu and Fe speciation to chalcopyrite bioleaching by *Acidithiobacillus ferrooxidans*. *Hydrometall.* 156, 40–46. <https://doi.org/10.1016/j.hydromet.2015.05.013>.
- Liu, T., Hu, S., Yuan, Z., Guo, J., 2023a. Microbial Stratification Affects Conversions of Nitrogen and methane in Biofilms Coupling Anammox and n-DAMO Processes. *Environ. Sci. Technol.* 57, 4608–4618. <https://doi.org/10.1021/acs.est.2c07294>.
- Liu, T., Hu, S., Yuan, Z., Guo, J., 2023b. Simultaneous dissolved methane and nitrogen removal from low-strength wastewater using anaerobic granule-based sequencing batch reactor. *Water Res.* 242, 120194. <https://doi.org/10.1016/j.watres.2023.120194>.
- Liu, T., Hu, S., Yuan, Z., Guo, J., 2019. High-level nitrogen removal by simultaneous partial nitrification, anammox and nitrite/nitrate-dependent anaerobic methane oxidation. *Water Res.* 166, 115057. <https://doi.org/10.1016/j.watres.2019.115057>.
- Lu, Y., Liu, T., Hu, S., Yuan, Z., Dwyer, J., Akker, B.V.D., Lloyd, J., Guo, J., 2024. Coupling Partial Nitrification, Anammox and n-DAMO in a membrane aerated biofilm reactor for simultaneous dissolved methane and nitrogen removal. *Water Res.* 255, 121511. <https://doi.org/10.1016/j.watres.2024.121511>.
- Mailler, R., Gasperi, J., Chebbo, G., Rocher, V., 2014. Priority and emerging pollutants in sewage sludge and fate during sludge treatment. *Waste Manag.* 34, 1217–1226. <https://doi.org/10.1016/j.wasman.2014.03.028>.
- Meng, J., Hu, Z., Wang, Z., Hu, S., Liu, Y., Guo, H., Li, J., Yuan, Z., Zheng, M., 2022. Determining Factors for Nitrite Accumulation in an Acidic Nitrifying System: Influent ammonium Concentration, Operational pH, and Ammonia-Oxidizing Community. *Environ. Sci. Technol.* 56, 11578–11588. <https://doi.org/10.1021/acs.est.1c07522>.
- Pathak, A., Dastidar, M.G., Sreekrishnan, T.R., 2009. Bioleaching of heavy metals from sewage sludge: a review. *J. Environ. Manage.* 90, 2343–2353. <https://doi.org/10.1016/j.jenvman.2008.11.005>.
- Raghoebarsing, A.A., Pol, A., van de Pas-Schoonen, K.T., Smolders, A.J.P., Ettwig, K.F., Rijpstra, W.L.C., Schouten, S., Damsté, J.S.S., Op den Camp, H.J.M., Jetten, M.S.M., Strous, M., 2006. A microbial consortium couples anaerobic methane oxidation to denitrification. *Nature* 440, 918–921. <https://doi.org/10.1038/nature04617>.
- Smith, S.R., 2009. A critical review of the bioavailability and impacts of heavy metals in municipal solid waste composts compared to sewage sludge. *Environ. Int.* 35, 142–156. <https://doi.org/10.1016/j.envint.2008.06.009>.
- Tou, F., Yang, Y., Feng, J., Niu, Z., Pan, H., Qin, Y., Guo, X., Meng, X., Liu, M., Hochella, M.F., 2017. Environmental Risk Implications of Metals in Sludges from Waste Water Treatment Plants: the Discovery of Vast Stores of Metal-Containing Nanoparticles. *Environ. Sci. Technol.* 51, 4831–4840. <https://doi.org/10.1021/acs.est.6b05931>.
- Wang, C., Shao, N., Xu, J., Zhang, Z., Cai, Z., 2020. Pollution emission characteristics, distribution of heavy metals, and particle morphologies in a hazardous waste incinerator processing phenolic waste. *J. Hazard. Mater.* 388, 121751. <https://doi.org/10.1016/j.jhazmat.2019.121751>.
- Wang, F., Yu, J., Xiong, W., Xu, Y., Chi, R., 2018. A two-step leaching method designed based on chemical fraction distribution of the heavy metals for selective leaching of Cd, Zn, Cu, and Pb from metallurgical sludge. *Environ. Sci. Pollut. Res.* 25, 1752–1765. <https://doi.org/10.1007/s11356-017-0471-7>.
- Wang, Z., Lu, X., Zhang, X., Yuan, Z., Zheng, M., Hu, S., 2024. Ammonium-based bioleaching of toxic metals from sewage sludge in a continuous bioreactor. *Water Res.* 256, 121651. <https://doi.org/10.1016/j.watres.2024.121651>.
- Wang, Z., Ni, G., Maulani, N., Xia, J., De Clippeleir, H., Hu, S., Yuan, Z., Zheng, M., 2021a. Stoichiometric and kinetic characterization of an acid-tolerant ammonia oxidizer 'Candidatus Nitrosoglobus'. *Water Res.* 196, 117026. <https://doi.org/10.1016/j.watres.2021.117026>.
- Wang, Z., Ni, G., Xia, J., Song, Y., Hu, S., Yuan, Z., Zheng, M., 2021b. Bioleaching of toxic metals from anaerobically digested sludge without external chemical addition. *Water Res.* 200, 117211.
- Yakameran, E., Ari, A., Ayyün, A., 2021. Land application of municipal sewage sludge: Human health risk assessment of heavy metals. *J. Clean. Prod.* 319, 128568. <https://doi.org/10.1016/j.jclepro.2021.128568>.
- Zhang, G., Hai, J., Ren, M., Zhang, S., Cheng, J., Yang, Z., 2013. Emission, Mass Balance, and distribution Characteristics of PCDD/Fs and Heavy Metals during Cocombustion of Sewage Sludge and coal in Power Plants. *Environ. Sci. Technol.* 47, 2123–2130. <https://doi.org/10.1021/es304127k>.
- Zhang, M., Huang, W., Zhang, L., Feng, Z., Zuo, Y., Xie, Z., Xing, W., 2024. Nitrite-dependent anaerobic methane oxidation (N-DAMO) in global aquatic environments: a review. *Sci. Total Environ.* 921, 171081. <https://doi.org/10.1016/j.scitotenv.2024.171081>.
- Zhang, Q., Hu, J., Lee, D.-J., Chang, Y., Lee, Y.-J., 2017. Sludge treatment: current research trends. *Bioresour. Technol.* 243, 1159–1172. <https://doi.org/10.1016/j.biortech.2017.07.070>.